Atmos. Chem. Phys. Discuss., 10, 21237–21257, 2010
www.atmos-chem-phys-discuss.net/10/21237/2010/
doi:10.5194/acpd-10-21237-2010

Atmospheric Chemistry and Physics Discussions

Characterization of high-resolution aerosol mass spectra of primary organic aerosol emissions from Chinese cooking and biomass burning

L.-Y. He[1], Y. Lin[1], X.-F. Huang[1], S. Guo[2], L. Xue[1], Q. Su[1], M. Hu[2], S.-J. Luan[1], and Y.-H. Zhang[2]

[1]Key Laboratory for Urban Habitat Environmental Science and Technology, School of Environment and Energy, Peking University Shenzhen Graduate School, Shenzhen, China
[2]State Key Joint Laboratory of Environmental Simulation and Pollution Control, College of Environmental Sciences and Engineering, Peking University, Beijing, China

Received: 19 August 2010 – Accepted: 1 September 2010 – Published: 7 September 2010

Correspondence to: X.-F. Huang (huangxf@pku.edu.cn)

Published by Copernicus Publications on behalf of the European Geosciences Union.

Abstract

Aerosol Mass Spectrometer (AMS) has proved to be a powerful tool to measure submicron particulate composition with high time resolution. Factor analysis of mass spectra (MS) collected worldwide by AMS demonstrates that submicron organic aerosol (OA) is usually composed of several major components, such as oxygenated (OOA), hydrocarbon-like (HOA), biomass burning (BBOA), and other primary OA. In order to help interpretation of component MS from factor analysis of ambient OA datasets, AMS measurement of different primary sources is required for comparison. Such work, however, has been very scarce in the literature, especially for high resolution MS (HR-MS) measurement, which performs improved characterization by separating the ions of different elemental compositions at each *m/z* in comparison with unit mass resolution MS (UMR-MS) measurement. In this study, primary emissions from four types of Chinese cooking (CC) and six types of biomass burning (BB) were simulated systemically and measured using an Aerodyne High-Resolution Time-of-Flight AMS (HR-ToF-AMS). The MS of the CC emissions show high similarity with *m/z* 41 and *m/z* 55 being the highest signals; the MS of the BB emissions also show high similarity with *m/z* 29 and *m/z* 43 being the highest signals. The MS difference between the CC and BB emissions is much bigger than that between different CC (or BB) types, especially for the HR-MS. The O/C ratio of OA ranges from 0.08 to 0.13 for the CC emissions while from 0.18 to 0.26 for the BB emissions. The ions of *m/z* 43, *m/z* 44, *m/z* 57, and *m/z* 60, usually used as tracer ions in AMS measurement, were examined for their HR-MS characteristics in the CC and BB emissions. Moreover, the MS of the CC and BB emissions are also used to compare with component MS from factor analysis of ambient OA datasets observed in China, as well as with other AMS measurements of primary sources in the literature. The MS signatures of cooking and biomass burning emissions revealed in this study can be used as important reference in factor analysis of ambient OA datasets, especially for the relevant studies in East Asia.

ACPD

10, 21237–21257, 2010

1 Introduction

Atmospheric aerosols are important because of their effects on climate, health, visibility and ecosystems. Organic aerosol (OA) is a major type of submicron aerosols and comes from various natural and anthropogenic sources, including both primary organic aerosol (POA) emitted directly as particles and secondary organic aerosol (SOA) photochemically formed from volatile organic compounds (VOCs) in the atmosphere. Due to the high complexity of OA composition, only ~10% of its mass has been identified as specific compounds (Rogge et al., 1993; Simoneit et al., 2004). Up to now, the primary sources and secondary formation mechanisms of OA are still quite uncertain.

In recent years, some research efforts have been focusing on classifying OA by category rather than identifying specific compounds and the technique of aerosol mass spectrometry has proved to be a promising one. The Aerosol Mass Spectrometer (AMS) manufactured by Aerodyne Inc. (Billerica, USA) can on-line determine submicron aerosols with high time resolution based on thermal vaporization and electron ionization (EI). Factor analysis of the mass spectra (MS) collected worldwide by AMS demonstrates that OA is usually composed of several major components, such as oxygenated (OOA), hydrocarbon-like (HOA), biomass burning (BBOA), and other primary organic aerosols (Zhang et al., 2007; Jimenez et al., 2009; Ng et al., 2010). The OOA has been revealed to be a good surrogate of SOA, while the HOA can be mostly attributed to combustion sources like vehicle exhaust. Cooking-related organic aerosol (COA) has also been identified to be significant recently by factor analysis of AMS datasets of some urban atmospheres (Allan et al., 2010; Huang et al., 2010).

In order to understand the MS signatures of different primary OA sources and thus help interpretation of MS component spectra from factor analysis of ambient datasets, direct AMS measurement of OA in different primary emissions is required for comparison. Mohr et al. (2009) recently reported the AMS measurement results of some typical motor vehicles, meat cooking, and trash burning, suggesting the MS signatures of these OA sources. Similar work, however, has been very scarce in the literature and

ACPD
10, 21237–21257, 2010

thus the MS signatures of different primary OA sources have not been established and confirmed yet for the AMS community. On the other hand, the characteristics of source emissions may vary geographically. For example, cooking emissions may have great local features in China due to the unique Chinese cooking methods and practices; burning of biomass fuel and crop waste is far more popular in rural areas in China than in developed countries. Since scarce sources and conditions were analyzed by AMS before, more experiments will be useful to form the generalities for different primary OA sources.

The purpose of this work is to characterize MS signatures of OA in primary emissions from Chinese cooking and biomass burning using an Aerodyne High-Resolution Time-of-Flight AMS (HR-ToF-AMS) of Peking University Shenzhen Graduate School. Compared to an Aerodyne unit mass-resolution (UMR) AMS, the HR-ToF-AMS is able to separate the ions of different elemental compositions at each *m/z* and thus performs improved characterization of OA and allows better factor analysis of MS with statistical techniques (DeCarlo et al., 2006; Docherty et al., 2008; Aiken et al., 2009). The MS measured for Chinese cooking and biomass burning are also used to compare with relevant component MS from factor analysis of ambient OA datasets observed in China, as well as with primary OA measurement results in the literature.

2 Experimental methods

2.1 Description of the combustion simulation system

The simulation of biomass burning (BB) and Chinese cooking (CC) emissions was performed in the Laboratory of Biomass Burning Simulation at Peking University Shenzhen Graduate School. The combustion simulation system in the laboratory, as shown in Fig. S1, was designed and constructed according to the one described in Zhang et al. (2008). A brief introduction of the system is given below. It consists of five main parts: a combustion pan, a hood, a dilution tunnel, a residence chamber, and several

ACPD
10, 21237–21257, 2010

sampling ports. All the relevant parts of the system were made of stainless steel to minimize potential absorption effect and artifacts. During a burning event, the biomass sample is placed on the combustion pan and ignited, the smoke emitted is collected together with ambient air by the hood above and then goes through the dilution tunnel, in which the smoke is diluted with zero air by a controlled ratio of 10∼100 times. After dilution, the smoke goes into the residence chamber, where it has to reside for about 30 s to cool down and become aged. The temperature in the residence chamber is less than 40 °C. The aged smoke is sampled through a port, further diluted by zero air, and then passes through a $PM_{2.5}$ cyclone to remove coarse particles before it is finally sampled by the HR-ToF-AMS. In order to simulate cooking emissions, the combustion pan is substituted by a hotplate, on which a frying pan is used to cook Chinese dishes.

2.2 Simulation of Chinese cooking and biomass burning emissions

Cooking emissions of four traditional Chinese dishes were simulated and analyzed in this study, including Hand-Ripped Cabbage (CC#1), Scrambled Eggs with Tomatoes (CC#2), Kung Pao Chicken (CC#3), and Spareribs Braised in Brown Sauce (CC#4). The ingredients used to cook these dishes are listed in Table S1. The temperature of the hotplate was set at 160∼180 °C for the cooking. Each dish was cooked for 2∼3 times for AMS measurement. Burning emissions of six types of biomass were simulated and analyzed, including wood of fir (BB#1), pine (BB#2), willow (BB#3), and wattle (BB#4), sugarcane leaves (BB#5), and rice straw (BB#6). These types of biomass are popular biofuel used for cooking and warming in China rural areas. On the other hand, rice straw and sugarcane leaves are two major types of agricultural waste in China rural areas and usually burned out intensively on the farmland after harvest, causing severe regional hazy days. The biomass materials used in this study were collected in the rural areas of Guangdong Province and Beijing and had all been air-dried before the experiments. About 0.5∼1.5 kg biomass was used for a single burning event. The burning of each biomass species was repeated for 2∼4 times, except only once for pine burning. All the experiments were carried out in December 2009 with a mean ambient temperature of 17 °C.

ACPD
10, 21237–21257, 2010

2.3 HR-ToF-AMS operation and data processing

An Aerodyne HR-ToF-AMS was used to on-line measure the submicron particles emitted from the sources. A detailed instrumental description of HR-ToF-AMS can be found in DeCarlo et al. (2006). The HR-ToF-AMS sampled isokinetically at a flow rate of 80 cc min^{-1}. During this study, the HR-ToF-AMS operated in a cycle of two modes, i.e., 1 min V-mode to obtain mass concentrations and 1 min W-mode to obtain high-resolution mass spectra. The HR-ToF-AMS was calibrated for inlet flow, ionization efficiency (IE), and particle sizing before and after the source measurements following the standard protocols (Jayne et al., 2000; Jimenez et al., 2003; Drewnick et al., 2005). The calibration of IE used size-selected pure ammonium nitrate particles and the size calibration was conducted using mono-disperse polystyrene latex spheres. Standard ToF-AMS data analysis software packages (including SQUIRREL version 1.49 and PIKA version 1.08) downloaded from the ToF-AMS-Resources webpage (http://cires.colorado.edu/jimenez-group/ToFAMSResources) were used to generate unit and high-resolution mass spectra from the V-mode and W-mode data, respectively, using the methods outlined in DeCarlo et al. (2006). Elemental analysis (C, H, O, and N) of the HR-MS was carried out with the methods described previously (Aiken et al., 2007, 2008). In the data processing, only the data with OA concentrations elevated largely from the baseline concentrations (~10 times) were used to generate representative HR-MS for different CC and BB emissions, which were calculated based on averages of 8~54 min data. Organic HR-MS were extracted from the dataset to discuss in the following sections. The time trends of OA concentrations during the measurement period are shown in Fig. S2.

ACPD
10, 21237–21257, 2010

3 Results and discussion

3.1 HR-MS profiles of OA from the sources

Figure 1 gives the average HR-MS of OA observed for the primary emissions of four types of Chinese cooking and six types of biomass burning, which are presented in the form of UMR-MS by stacking the ions of the same mass integer. All the ten MS are dominated by the ion series of $C_nH^+_{2n+1}$ and $C_mH_{2m+1}CO^+$ (*m/z* 29, 43, 57, 71, 85...) and $C_nH^+_{2n-1}$ and $C_mH_{2m-1}CO^+$ (*m/z* 41, 55, 69, 83...), indicating large presence of saturated alkanes, alkenes, and also possible long-chain fatty acids in the primary OA from the CC and BB emissions. However, the most prominent ions are different between the CC and BB emissions: *m/z* 41 and *m/z* 55 are the two most abundant ions for the CC emissions, while *m/z* 29 and *m/z* 43 are the most abundant ions for the BB emissions. In addition, there appears to be more mass distribution in the range of *m/z*>100 in the BB emissions than in the CC emissions.

The HR-MS of the CC emissions indicate that *m/z* 41 and *m/z* 55 are dominated by $C_3H^+_5$ and $C_4H^+_7$, respectively, both of which are fragments resulting from EI of unsaturated organic compounds. As unsaturated fatty acids were identified as abundant OA species from Chinese cooking emissions by GC-MS analysis (He et al., 2004; Zhao et al., 2007), the great presence of *m/z* 41 and *m/z* 55 is a reasonable result of the AMS measurement. A recent AMS measurement of primary cooking emissions (heating of seed oils) by Allan et al. (2010) also revealed the highest ions of *m/z* 41 and *m/z* 55 in the UMR-MS profiles, which is consistent with our results. However, the AMS measurement of primary cooking emissions (meat charbroiling) by Mohr et al. (2009) shows the highest ions of *m/z* 43 and *m/z* 55 in the UMR-MS profiles. Our results suggest that OA generated due to frying is more important than OA generated from meat charbroiling in Chinese cooking emissions. This is consistent with the fact that frying is a major process for the cooking of the four Chinese dishes, as well as for the cooking of most Chinese dishes.

ACPD
10, 21237–21257, 2010

The HR-MS of the BB emissions indicate that the prominent signals of *m/z* 29 and *m/z* 43 are mainly due to the large presence of the oxygen-containing ions of CHO^+ and $C_2H_3O^+$, respectively, which are more abundant than the hydrocarbon ions at the same mass integers. In fact, not only *m/z* 29 and *m/z* 43 but also most other mass integers are largely contributed by oxygen-containing ions. The high fractions of oxygen-containing ions in the HR-MS of the BB emissions are consistent with previous findings that polar, oxygen-containing, and water-soluble organic compounds dominate primary aerosols emitted from biomass burning (Novakov and Corrigan, 1996; Narukawa et al., 1999). There also exist significant amounts of *m/z* 44 and *m/z* 60, the two tracer ions for OOA and BBOA, respectively, which are discussed in Sect. 3.4. These characteristics are generally consistent with the HR-MS of OA from pine burning reported by Aiken et al. (2008, 2009) and the UMR-MS of OA from chestnut burning reported by Alfarra et al. (2007). This study consolidates the MS signatures of OA from primary BB emissions by more sample types. The MS signal fractions of *m/z*>100 are 11∼13% for the six BB types, significantly higher than 5∼7% for the four CC types, which implies that OA from primary BB emissions contains high molecular weight organic compounds. This can be supported by previous findings that biomass burning aerosol contains a large amount of humic-like substances (Mayol-Bracero et al., 2002; Gelencser et al., 2000; Lin et al., 2010).

The HR-MS observed for the primary CC and BB emissions are also used to compare with two component HR-MS of the cooking-related organic aerosol (COA) and the biomass burning organic aerosol (BBOA) (as shown in Fig. 1) resolved by positive matrix factorization (PMF) analysis of ambient HR-MS datasets measured by our group. The COA was identified in OA of urban Beijing in summer 2008 (Huang et al., 2010) and the BBOA was identified in OA of urban Shenzhen in fall 2009 (He et al., 2010). It is seen in Fig. 1 that the major MS signatures of the COA and BBOA match those of the CC and BB emissions measured in this study, respectively, such as the most prominent ions and fractions of oxygen-containing ions, supporting the representativeness of the COA and BBOA in the corresponding AMS-PMF studies. The MS of the CC and BB

ACPD
10, 21237–21257, 2010

emissions measured in this study are significantly different from the MS from vehicle exhaust and plastic burning, which typically have the highest ion of *m/z* 43 (Mohr et al., 2009), and also greatly different from the MS of OOA, which typically have the highest ion of *m/z* 44 (Zhang et al., 2007; Ng et al., 2010).

3.2 Correlation relationship of the HR-MS profiles of sources

As general evaluation of the similarity between the MS profiles of the different sources measured in this study, in the forms of both UMR-MS and HR-MS, their correlation coefficients were calculated and summarized in Table 1. The trends in correlation coefficient for UMR-MS and HR-MS are found to be well correlated ($R^2 = 0.97$). In terms of either UMR-MS or HR-MS, the four types of CC emissions show high inter-correlation relationship ($R^2 \geqq 0.94$) and it is also the case for the six types of BB emissions ($R^2 \geqq 0.75$), indicating good consistency of the MS profiles of different types of CC (or BB) emissions. For the correlation relationship between a CC source and a BB source, R^2 ranges from 0.54~0.92 for UMR-MS with a mean value of 0.77, while ranges from 0.32~0.85 for HR-MS with a mean value of 0.63. This result has two main implications: firstly, the MS difference between CC and BB emissions is much bigger than that between different CC (or BB) types, therefore BB and CC emissions are very likely to be separated into two OA components in MS factor analysis of ambient datasets; secondly, there is more difference between CC and BB emissions in HR-MS than in UMR-MS, which would allow better separation of these two primary OA sources in MS factor analysis of ambient datasets, showing the advantage of utilizing a HR-ToF-AMS. In terms of either UMR-MS or HR-MS, the two OA components derived from ambient datasets, i.e., the COA and BBOA, show significantly higher correlation relationship with the CC and BB emissions, respectively, also shown in Table 1, strongly confirming their representativeness.

ACPD
10, 21237–21257, 2010

3.3 Elemental composition of OA from the sources

The elemental compositions of the different CC and BB emissions are presented as inserted plots in Fig. 1. Figure 2 compares their elemental ratios of H/C, O/C, and N/C, as well as those of the COA and BBOA. Compared to the CC emissions and COA, the BB emissions and BBOA have higher O/C but lower H/C. The O/C ranges from 0.18 to 0.26 for the six types of BB emissions while from 0.08 to 0.13 for the four types of CC emissions. Also based on HR-ToF-AMS measurement, Mohr et al. (2009) reported O/C of 0.11 and 0.14 for cooking of fatty hamburger and chicken without skin, respectively; Aiken et al. (2008) reported O/C of 0.31 and 0.42 for lodgepole pine and sage/rabbitbrush burning, respectively. Compared to their results, our measurements observed similar O/C levels for CC and BB emissions, but with broader ranges due to more sample types tested. Combining the findings in this study and in the literature, it is safe to say that OA from biomass burning emissions would have significantly higher O/C levels than OA from cooking emissions. In addition, all the CC and BB emissions measured in this study have O/C higher than vehicle exhaust and plastic burning (0.03~0.04) but lower than OOA (0.5~1) (Mohr et al., 2009; Jimenez et al., 2009). It is worth noting that in previous OA factor analysis of ambient datasets, HOA was resolved with O/C of 0.06~0.17 (Aiken et al., 2008, 2009; Huang et al., 2010), which are significantly higher than 0.03~0.04 directly measured for vehicle exhaust (Mohr et al., 2009) and overlap with the O/C range of cooking emissions. A very recent study found that semi-volatile organic compounds (SVOCs) in vehicle emissions can be effectively photo-oxidized with a cycling between the gas and particle phases, which creates more oxygenated OA but little new OA mass (Miracolo et al., 2010). Therefore, once entering the atmosphere, fresh HOA in vehicle exhaust is supposed to be effectively photo-oxidized to increase its O/C to a similar level to that of cooking emissions. The N/C is small (0.008~0.018) for all the CC and BB emissions. The BBOA identified in Shenzhen, however, has a uniquely high N/C of 0.06, implying that unknown high N-containing emissions might be involved in the BBOA. Due to the small

ACPD
10, 21237–21257, 2010

factions of nitrogen in the OA, the variation of OM/OC (organic matter mass to organic carbon mass) among different source types resembles that of O/C, ranging from 1.26 to 1.33 for the four types of CC emissions and from 1.39~1.49 for the six types of BB emissions.

3.4 Characteristics of tracer ions in MS

The UMR ions of *m/z* 43, *m/z* 44, *m/z* 57, and *m/z* 60 have been usually used as tracer ions in MS of total OA, OOA, HOA, and BBOA, respectively, because they typically correlate well with these OA components in statistical analysis of ambient datasets (Zhang et al., 2005; Alfarra et al., 2007; Ng et al., 2010). Therefore, it is necessary and interesting to examine the patterns of these ions in the CC and BB emissions measured in this study to explore their representativeness and possible interferences in the case of cooking and biomass burning OA.

Taking advantage of the HR-MS in this study, it is possible to first examine what ions comprise these four UMR ions. Figure 3 compares the compositions of *m/z* 43, *m/z* 44, *m/z* 57, and *m/z* 60 for the BB and CC emissions, as well as those of the COA and BBOA. For *m/z* 43, $C_2H_3O^+$ and $C_3H_7^+$ are always the two major ions at this mass integer. However, the abundance of $C_3H_7^+$ in the CC emissions is much higher than that of $C_2H_3O^+$, while in the BB emissions the abundance of $C_3H_7^+$ is similar to or even lower than that of $C_2H_3O^+$. For *m/z* 44, CO_2^+ is always the dominant ion, denoting high accordance of *m/z* 44 and CO_2^+. The UMR ion of *m/z* 57 has been regarded as a good reference for HOA emitted from primary combustion sources, which seems to be the case for the CC emissions but questionable for the BB emissions. The abundance of $C_4H_9^+$ in the CC emissions is much higher than that of $C_3H_5O^+$, while in the BB emissions the abundance of $C_4H_9^+$ is similar to or even lower than that of $C_3H_5O^+$. Aiken et al. (2009) reported a HR-MS of pine burning, in which $C_3H_5O^+$ is also higher than $C_4H_9^+$. This result suggests that *m/z* 57 in UMR-MS may not be a good tracer ion for hydrocarbons in biomass burning emissions. For *m/z* 60, it is always dominated by $C_2H_4O_2^+$, benefiting the use of this UMR ion as tracer.

ACPD
10, 21237–21257, 2010

Figure 4 compares the signal abundances of *m/z* 43, *m/z* 44, *m/z* 57, and *m/z* 60 in UMR-MS of OA from different primary sources as in this study and reported in the literature, in order to extract general characteristics of these ions in cooking and biomass burning emissions. The signal abundances of *m/z* 43 are similar for cooking and biomass burning emissions, in the range of 0.05~0.10, but they are slightly lower than those from vehicle exhaust and plastic burning. The signal abundances of *m/z* 44 generally show higher values for biomass burning emissions (0.02~0.05) than those from cooking emissions (≤0.02), vehicle exhaust, and plastic burning. For *m/z* 57, the signal abundances are similar for cooking and biomass burning emissions, in the range of 0.02~0.06, but they are significantly lower than those from vehicle exhaust and plastic burning. As *m/z* 57 and *m/z* 43 from vehicle exhaust and plastic burning are dominated by hydrocarbon ions rather than oxygen-containing ions (Mohr et al., 2009), their higher signals suggest that hydrocarbons are more emitted from vehicles and plastic burning. The ion of *m/z* 60 ($C_2H_4O_2^+$) was detected with lower signals for cooking emissions and almost no signals for vehicle exhaust and plastic burning, while it exists with higher signals for biomass burning emissions (0.012~0.057).

The above analysis of the tracer ions in OA UMR-MS from different primary sources may indicate that: 1. the signals of *m/z* 43 are less variable among different primary sources; 2. the signals of *m/z* 44 from biomass burning emissions are uniquely higher than other primary sources and may interfere the denoting of *m/z* 44 for SOA during biomass burning events; 3. *m/z* 57 is more characteristic for vehicle hydrocarbon emissions; 4. although *m/z* 60 is more significantly emitted from biomass burning, it also exists with detectable amounts in cooking emissions.

4 Conclusions

Primary emissions from four types of Chinese cooking (CC) and six types of biomass burning (BB) were simulated and measured using an Aerodyne HR-ToF-AMS. All the MS profiles observed are dominated by ion fragments from saturated alkanes, alkenes,

ACPD
10, 21237–21257, 2010

as well as possible long-chain fatty acids. The MS of the CC emissions show high similarity with *m/z* 41 and *m/z* 55 being the most abundant signals; the MS of the BB emissions also show high similarity with *m/z* 29 and *m/z* 43 being the most abundant signals. The MS difference between the CC and BB emissions is much bigger than that between different CC (or BB) types, especially for HR-MS, therefore cooking and biomass burning emissions are very likely to be separated into two components in MS factor analysis of ambient OA datasets. The O/C ratio of OA ranges from 0.08 to 0.13 for the CC emissions while from 0.18 to 0.26 for the BB emissions. The MS signatures of the COA and BBOA resolved by PMF analysis of ambient OA datasets in China field campaigns well match those of the CC and BB emissions, respectively, strongly supporting their representativeness in the corresponding AMS-PMF studies. HR-MS analysis indicates that the signals of *m/z* 44 and *m/z* 60 are mostly from CO_2^+ and $C_2H_4O_2^+$, respectively, in the CC and BB emissions. The signals of *m/z* 44 from biomass burning emissions are uniquely higher than other primary sources. The ion of *m/z* 60, typically used as the tracer ion for biomass burning, also exists significantly in cooking emissions. The MS signatures of cooking and biomass burning emissions revealed in this study will help interpretation of component MS from factor analysis of ambient OA datasets.

Supplementary material related to this article is available online at: http://www.atmos-chem-phys-discuss.net/10/21237/2010/acpd-10-21237-2010-supplement.pdf.

Acknowledgements. This work was supported by the "863" project (2006AA06A308, 2006AA06A309) from the Ministry of Science and Technology of China, the Science and Technology Plan Project of Shenzhen Municipality (CXB200903090046A), and the National Natural Science Foundation of China (20777001).

ACPD
10, 21237–21257, 2010

References

Aiken, A. C., DeCarlo, P. F., and Jimenez, J. L.: Elemental analysis of organic species with electron ionization high-resolution mass spectrometry, Anal. Chem., 79, 8350–8358, 2007.

Aiken, A. C., Decarlo, P. F., Kroll, J. H., et al.: O/C and OM/OC ratios of primary, secondary, and ambient organic aerosols with high-resolution time-of-flight aerosol mass spectrometry, Environ. Sci. Technol., 42, 4478–4485, 2008.

Aiken, A. C., Salcedo, D., Cubison, M. J., Huffman, J. A., DeCarlo, P. F., Ulbrich, I. M., Docherty, K. S., Sueper, D., Kimmel, J. R., Worsnop, D. R., Trimborn, A., Northway, M., Stone, E. A., Schauer, J. J., Volkamer, R. M., Fortner, E., de Foy, B., Wang, J., Laskin, A., Shutthanandan, V., Zheng, J., Zhang, R., Gaffney, J., Marley, N. A., Paredes-Miranda, G., Arnott, W. P., Molina, L. T., Sosa, G., and Jimenez, J. L.: Mexico City aerosol analysis during MILAGRO using high resolution aerosol mass spectrometry at the urban supersite (T0) – Part 1: Fine particle composition and organic source apportionment, Atmos. Chem. Phys., 9, 6633–6653, doi:10.5194/acp-9-6633-2009, 2009.

Alfarra, M. R., Prevot, A. S. H., Szidat, S., et al.: Identification of the mass spectral signature of organic aerosols from wood burning emissions, Environ. Sci. Technol., 41, 5770–5777, 2007.

Allan, J. D., Williams, P. I., Morgan, W. T., Martin, C. L., Flynn, M. J., Lee, J., Nemitz, E., Phillips, G. J., Gallagher, M. W., and Coe, H.: Contributions from transport, solid fuel burning and cooking to primary organic aerosols in two UK cities, Atmos. Chem. Phys., 10, 647–668, doi:10.5194/acp-10-647-2010, 2010.

DeCarlo, P. F., Kimmel, J. R., Trimborn, A., et al.: Field-Deployable, High-Resolution Time-of-Flight Aerosol Mass Spectrometer, Anal. Chem., 78, 8281–8289, 2006.

Docherty, K. S., Stone, E. A., Ulbrich, I. M., et al.: Apportionment of Primary and Secondary Organic Aerosols in Southern California during the 2005 Study of Organic Aerosols in Riverside (SOAR-1), Environ. Sci. Technol., 42, 7655–7662, 2008.

Drewnick, F., Hings, S. S., DeCarlo, P., et al.: A new time-of-flight aerosol mass spectrometer (TOF-AMS) – Instrument description and first field deployment, Aerosol. Sci. Tech., 39, 637–658, 2005.

Gelencser, A., Hoffer, A., Krivacsy, Z., et al.: On the possible origin of humic matter in fine continental aerosol, J. Geophys. Res.-Atmos., 107, 4137, doi:10.1029/2001JD001299, 2000.

He, L. Y., Hu, M., Huang, X. F., et al.: Measurement of emissions of fine particulate organic

ACPD
10, 21237–21257, 2010

matter from Chinese cooking, Atmos. Environ., 38, 6557–6564, 2004.
He, L. Y., Xue, L., Huang, X. F., et al.: Submicron aerosol analysis and organic source apportionment in a coastal urban atmosphere in South China using high-resolution aerosol mass spectrometry, J. Geophys. Res.-Atmos., in review, 2010.
Huang, X.-F., He, L.-Y., Hu, M., Canagaratna, M. R., Sun, Y., Zhang, Q., Zhu, T., Xue, L., Zeng, L.-W., Liu, X.-G., Zhang, Y.-H., Jayne, J. T., Ng, N. L., and Worsnop, D. R.: Highly time-resolved chemical characterization of atmospheric submicron particles during 2008 Beijing Olympic Games using an Aerodyne High-Resolution Aerosol Mass Spectrometer, Atmos. Chem. Phys. Discuss., 10, 13219–13251, doi:10.5194/acpd-10-13219-2010, 2010.
Jayne, J. T., Leard, D. C., Zhang, X. F., et al.: Development of an aerosol mass spectrometer for size and composition analysis of submicron particles, Aerosol. Sci. Tech., 33, 49–70, 2000.
Jimenez, J. L., Canagaratna, M. R., Donahue, N. M., et al.: Evolution of organic aerosols in the atmosphere, Science, 326, 1525–1529, 2009.
Jimenez, J. L., Jayne, J. T., Shi, Q., et al.: Ambient aerosol sampling using the Aerodyne Aerosol Mass Spectrometer, J. Geophys. Res.-Atmos., 108, 8425, doi:10.1029/2001JD001213, 2003.
Lin, P., Huang, X. F., He, L. Y., et al.: Abundance and size distribution of HULIS in ambient aerosols at a rural site in South China, J. Aerosol Sci., 41, 74–87, 2010.
Mayol-Bracero, O. L., Guyon, P., Graham, B., et al.: Water-soluble organic compounds in biomass burning aerosols over Amazonia. 2 Apportionment of the chemical composition and importance of the polyacidic fraction, J. Geophys. Res.-Atmos., 107, 8091, doi:10.1029/2001JD000522, 2002.
Miracolo, M. A., Presto, A. A., Lambe, A. T., et al.: Photo-Oxidation of Low-Volatility Organics Found in Motor Vehicle Emissions: Production and Chemical Evolution of Organic Aerosol Mass, Environ. Sci. Technol., 44, 1638–1643, 2010.
Mohr, C., Huffman, J. A., Cubison, M. J., et al.: Characterization of Primary Organic Aerosol Emissions from Meat Cooking, Trash Burning, and Motor Vehicles with High-Resolution Aerosol Mass Spectrometry and Comparison with Ambient and Chamber Observations, Environ. Sci. Technol., 43, 2443–2449, 2009.
Narukawa, M., Kawamura, K., Takeuchi, N., et al: Distribution of dicarboxylic acids and carbon isotopic compositions in aerosols from 1997 Indonesian forest fires, Geophys. Res. Lett., 26, 3101–3104, 1999.
Ng, N. L., Canagaratna, M. R., Zhang, Q., Jimenez, J. L., Tian, J., Ulbrich, I. M., Kroll, J. H.,

ACPD
10, 21237–21257, 2010

Docherty, K. S., Chhabra, P. S., Bahreini, R., Murphy, S. M., Seinfeld, J. H., Hildebrandt, L., Donahue, N. M., DeCarlo, P. F., Lanz, V. A., Prévôt, A. S. H., Dinar, E., Rudich, Y., and Worsnop, D. R.: Organic aerosol components observed in Northern Hemispheric datasets from Aerosol Mass Spectrometry, Atmos. Chem. Phys., 10, 4625–4641, doi:10.5194/acp-10-4625-2010, 2010.

Novakov, T. and Corrigan, C. E.: Cloud condensation nucleus activity of the organic component of biomass smoke particles, Geophys. Res. Lett., 23, 2141–2144, 1996.

Rogge, W. F., Mazurek, M. A., Hildemann, L. M., et al.: Quantification of urban organic aerosols at a molecular level: Identification, abundance and seasonal variation, Atmos. Environ. Part A, 27, 1309–1330, 1993.

Simoneit, B. R. T., Kobayashi, M., Mochida, M., et al.: Composition and major sources of organic compounds of aerosol particulate matter sampled during the ACE-Asia campaign, J. Geophys. Res., 109, D19S10, doi:10.1029/2004JD004598, 2004.

Zhang, Q., Alfarra, M. R., Worsnop, D. R., et al.: Deconvolution and quantification of hydrocarbon-like and oxygenated organic aerosols based on aerosol mass spectrometry, Environ. Sci. Technol., 39, 4938–4952, 2005.

Zhang, Q., Jimenez, J. L., Canagaratna, M. R., et al.: Ubiquity and dominance of oxygenated species in organic aerosols in anthropogenically-influenced Northern Hemisphere midlatitudes, Geophys. Res. Lett., 34, L13801, doi:10.1029/2007GL029979, 2007.

Zhang, Y. X., Schauer, J. J., Zhang, Y. H., et al.: Characteristics of Particulate Carbon Emissions from Real-World Chinese Coal Combustion, Environ. Sci. Technol., 42, 5068–5073, 2008.

Zhao, Y. L., Hu, M., Slanina, S., and Zhang, Y. H.: Chemical compositions of fine particulate organic matter emitted from Chinese cooking, Environ. Sci. Technol., 41, 99–105, 2007.

ACPD
10, 21237–21257, 2010

Table 1. Correlation coefficients (R^2) between UMR-MS (and HR-MS, in grey cells) profiles of different source emissions and PMF factors.

UMR	CC#1	CC#2	CC#3	CC#4	BB#1	BB#2	BB#3	BB#4	BB#5	BB#6	COA	BBOA	R^2
CC#1	1.00	0.98	0.97	0.94	0.59	0.54	0.83	0.67	0.73	0.79	0.93	0.46	CC#1
CC#2	0.96	1.00	0.99	0.97	0.70	0.66	0.91	0.78	0.83	0.88	0.94	0.59	CC#2
CC#3	0.97	0.98	1.00	0.97	0.70	0.66	0.92	0.79	0.84	0.89	0.93	0.61	CC#3
CC#4	0.95	0.97	0.97	1.00	0.74	0.68	0.90	0.80	0.85	0.88	0.90	0.60	CC#4
BB#1	0.41	0.54	0.50	0.54	1.00	0.96	0.89	0.98	0.93	0.87	0.62	0.89	BB#1
BB#2	0.32	0.46	0.42	0.44	0.94	1.00	0.85	0.96	0.94	0.87	0.55	0.88	BB#2
BB#3	0.75	0.85	0.84	0.83	0.84	0.75	1.00	0.94	0.96	0.97	0.84	0.80	BB#3
BB#4	0.51	0.64	0.62	0.64	0.97	0.94	0.92	1.00	0.98	0.95	0.68	0.89	BB#4
BB#5	0.62	0.74	0.73	0.74	0.89	0.87	0.95	0.97	1.00	0.98	0.74	0.86	BB#5
BB#6	0.70	0.81	0.81	0.80	0.81	0.78	0.95	0.91	0.96	1.00	0.79	0.81	BB#6
COA	0.86	0.87	0.89	0.90	0.44	0.32	0.74	0.52	0.64	0.69	1.00	0.48	COA
BBOA	0.18	0.31	0.28	0.29	0.82	0.84	0.59	0.78	0.69	0.61	0.20	1.00	BBOA
R^2	CC#1	CC#2	CC#3	CC#4	BB#1	BB#2	BB#3	BB#4	BB#5	BB#6	COA	BBOA	HR

ACPD
10, 21237–21257, 2010

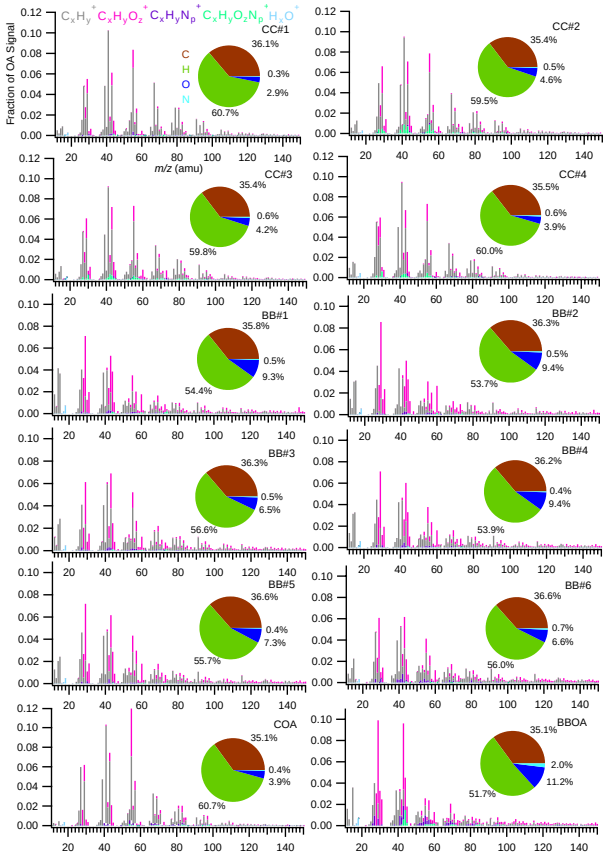

Fig. 1. The HR-MS profiles of OA from ten types of Chinese cooking and biomass burning emissions and two PMF-resolved OA factors (Hand-Ripped Cabbage (CC#1); Scrambled Eggs with Tomatoes (CC#2); Kung Pao Chicken (CC#3); Spareribs Braised in Brown Sauce (CC#4); fir (BB#1); pine (BB#2); willow (BB#3); wattle (BB#4); sugarcane leaves (BB#5); rice straw (BB #6); cooking-related OA in Beijing ambient (COA); biomass burning OA in Shenzhen ambient (BBOA)).

ACPD
10, 21237–21257, 2010

Characterization of high-resolution aerosol mass spectra

L.-Y. He et al.

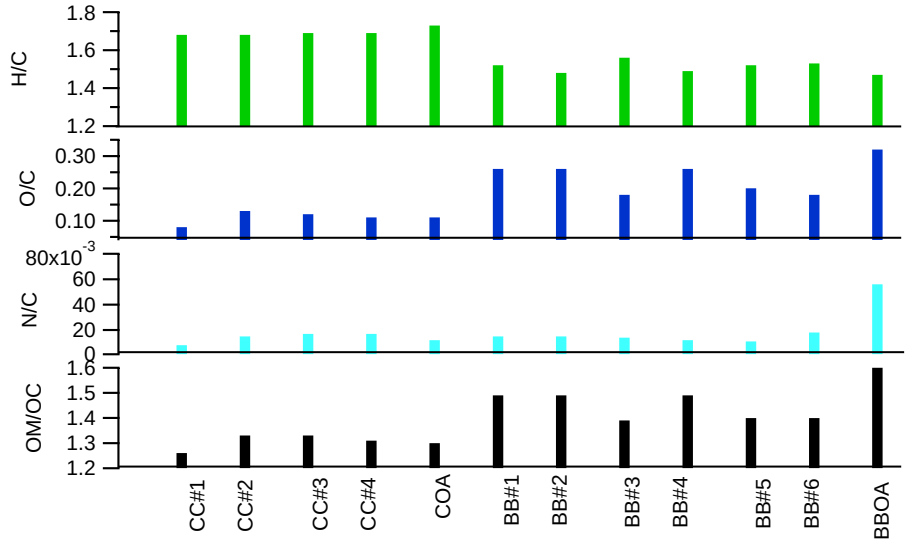

Fig. 2. Comparison of H/C, O/C, N/C, and OM/OC ratios of OA from ten types of Chinese cooking and biomass burning emissions and two PMF-resolved OA factors.

ACPD
10, 21237–21257, 2010

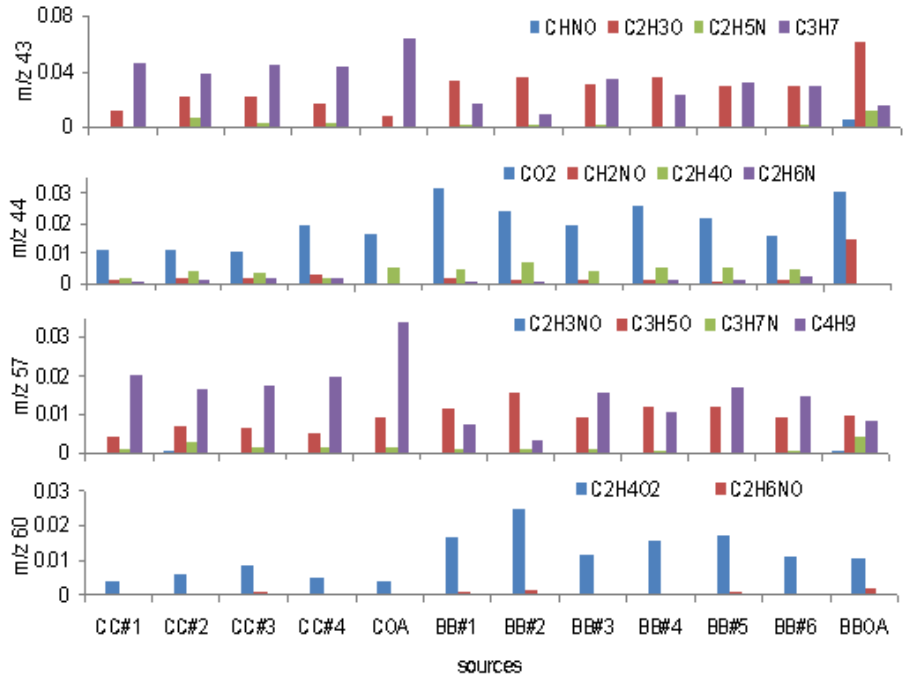

Fig. 3. Comparison of HR-MS ion signals at *m/z* 43, *m/z* 44, *m/z* 57, and *m/z* 60 of OA from ten types of Chinese cooking and biomass burning emissions and two PMF-resolved OA factors.

ACPD
10, 21237–21257, 2010

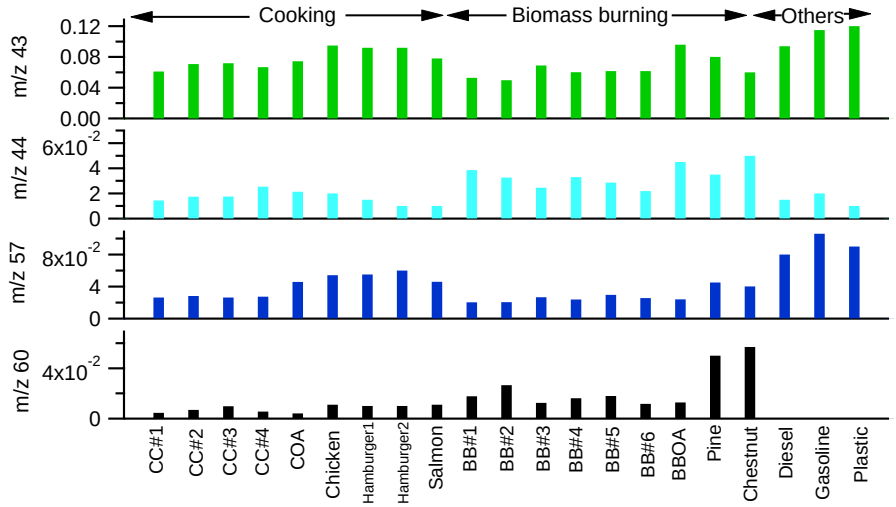

Fig. 4. Comparison of UMR-MS ion signals at *m/z* 43, *m/z* 44, *m/z* 57, and *m/z* 60 of OA from ten types of Chinese cooking and biomass burning emissions and two PMF-resolved OA factors, as well as those from other primary sources as reported in the literature (data source: chicken w/o skin, lean hamburger (#1), fatty hamburger (#2), salmon, diesel and gasoline engines, and plastic burning from Mohr et al., 2009; pine burning from Aiken et al., 2009; chestnut burning from Alfarra et al., 2007).

ACPD
10, 21237–21257, 2010